# Modeling of Reactivity Effects and Transient Behaviour of Large Sodium Fast Reactor

**Alexander Ponomarev**[1]
Paul Scherrer Institute (PSI)
Forschungsstrasse 111, 5232 Villigen PSI, Schweiz.PSI
alexander.ponomarev@psi.ch

**Konstantin Mikityuk**
Paul Scherrer Institute (PSI)
Forschungsstrasse 111, 5232 Villigen PSI, Schweiz.PSI
konstantin.mikityuk@psi.ch

## ABSTRACT

*In the paper the reactivity characteristics of the core of the large sodium fast reactor Superphénix (SPX) were evaluated and compared with available experimental data. The analysis was performed using the TRACE system code modified for the fast reactor applications. The simplified core model was developed aiming to overcome the lack of detailed information on design and realistic core conditions. Point kinetics neutronic model with all relevant reactivity feedbacks was used to calculate transient power. The paper focuses on challenging issue of modelling of the transient thermal responses of primary system structural elements resulting in reactivity feedbacks specific to such large fast reactor which cannot be neglected. For these effects, the model was equipped with dedicated heat structures to reproduce important feedbacks due to vessel wall, diagrid, strongback, control rod drive lines thermal expansion. Peculiarly, application of the model was considered for a whole range of core conditions from zero power to 100% nominal. The developed core model allowed reproducing satisfactorily the core reactivity balance between zero power at 180°C and full power conditions. Additionally, the reactivity coefficients k, g, h at*

[1] Corresponding author

This document is the accepted manuscript version of the following article:
Ponomarev, A., & Mikityuk, K. (2022). Modeling of reactivity effects and transient behavior of large sodium fast reactor. Journal of Nuclear Engineering and Radiation Science, 8(1), 011313 (7 pp.).
https://doi.org/10.1115/1.4051514

*three power levels (about 20, 50 and 80% of the nominal power) were calculated and satisfactory agreement with experimental measurements was also observed. The study demonstrated feasibility of application of relatively simple model with adjusted parameters for analysis of different conditions of very complex system. Reducing some differences with experimentally observed behaviour of feedback coefficients, would require more sophisticated approaches on fuel pin model, more detailed information on management of control rods during power rise, more complicated models of primary system, its structural elements and flow paths.*

## 1. INTRODUCTION

The Sodium-cooled Fast Reactor (SFR) technology with the total experience of more than 300 reactor-years relates to one of the most advanced and developed Generation-IV technologies [1]. It comprises a unique legacy of SFR developments and experimental data available from numerous experimental facilities and few industrial prototype reactors being operated in different countries [2].

Current work is devoted to the neutronics and thermal hydraulic transient analysis of the largest ever-built SFR – French Superphénix (SPX) reactor [3]. Considerable amount of experimental data were obtained during reactor operation that provides a unique basis for the validation of numerical codes for static and transient analysis. Within the ongoing Horizon-2020 ESFR-SMART project [4] a benchmark study has been initiated for evaluation of the core neutron physics characteristics and its transient behaviour [5]. Current study used the benchmark exercise basis for the analysis of the core reactivity balance and corresponding reactivity coefficients at core conditions from cold zero power to nominal power operation. A simplified three-channel model proposed within the ongoing benchmark study of SPX start-up transients was used. The model and assumptions developed in this study will be applied in the benchmark for analysis of particular transient conditions. The peculiarity of this study is application of a simplified model with fixed set of parameters, along with number of

assumptions applied for highly uncertain parameters, to reproduce a whole range of core conditions from zero power to 100% nominal. Essentially important feature of the model is account for SFR-specific reactivity effects related to thermal expansion of in-reactor structures which can not be neglected in such large core. Simulation results of modelling of reactivity change during transition from cold zero power to nominal operation, performed in the first part of the study, provide a basis for calculation of reactivity coefficients *k*, *g*, *h* measured during start-up tests. The study aims on evaluation of feasibility of the approaches on calculation of core reactivity and simulation of transient thermal response of in-reactor structures and provides new inputs for currently ongoing studies of the European SFR core behaviour within the ESFR-SMART project.

## 2. SUPERPHENIX REACTOR AND START-UP TESTS

The SPX reactor became the largest ever constructed liquid metal cooled fast breeder reactor [3]. Table 1 summarizes main parameters of the reactor at its start-up configuration. The MOX-fuelled core (Figure 1) consisting of about 360 fissile subassemblies (SAs) contains about 5.7 tons of plutonium and equipped with the breeder blanket zones. These are uranium oxide lower and upper axial breeder zones in the fissile SAs and a number of radial breeder SAs surrounding the fissile core.
The core criticality was achieved in 1985 followed by a number of experiments and tests, while the designed nominal power was reached in December 1986. Comprehensive measurements were gained during this phase of the start-up tests which included numerous tests carried out during few months of commissioning after the first core load. Different core characteristics such as the neutron fluxes, power distributions, the control rod worth, and the transient responses to a number of perturbations at different power level were analysed [6].

The published analysis of the experimental data and comparisons with calculations reported in [7-10] is of a great interest. In particular, a number of studies were devoted to prediction of core neutronics characteristics and transient response of

core neutronics, thermal hydraulics and mechanics to various perturbations during the start-up tests. Current paper addresses those tests related to evaluation of core reactivity characteristics and transient behaviour. Namely, in [9] the methodology of the experimental evaluation of the reactivity coefficients *k*, *g*, *h* is described and results of calculations are also presented. The corresponding set of three transients provides an interesting basis for validation of the calculation tools. The publication also includes a reactivity balance study, which provides an important information on core criticality and reactivity change within a wide range of core thermal and power conditions. Furthermore, in [10] three more transients were discussed providing further data for code validation.

## 3. MODELS

### 3.1. Code for simulations

The US NRC TRACE code, modified at PSI in order to model fast reactor specific features, was used to simulate transient thermal hydraulic and neutronic behaviour of the SPX core [11]. The current version of the code includes modifications of two-phase sodium flow option, fast reactor specific reactivity effects, new fuel performance model, etc. The code can be applied for analysis of a number of innovative reactor types (SFR, GFR, MSR) and broadly used for analysis of fast sodium systems in the past [12].
The neutronics parameters used for the transient calculations were evaluated with Serpent 2, 3D continuous-energy Monte Carlo neutron transport code for reactor physics application. The code has been developed at VTT Technical Research Centre of Finland since 2004 [13]. The continuous-energy ACE format data library JEFF-3.1.1, included in the installation package, was utilised. The library contains nuclear data at six temperatures between 300 and 1800 K.

### 3.2. Thermal hydraulic core model

A simplified primary system model describes the core represented by three channels connecting cold and hot plena. It employs specific boundary conditions at cold plenum inlet and hot plenum outlet (Figure 2). Inlet boundary condition is defined by providing

the inlet sodium temperature and mass flow rate. Outlet boundary condition is defined as constant pressure in the outlet plenum. The sodium flow in the inter-subassembly gap is neglected. This model has been applied in [14] in the framework of the benchmark activity. In particular, it was stated that the three-channel model supplied with core-averaged reactivity coefficients satisfactorily represents the core transient behaviour. The three channel model was used in the current work. It includes one individual channel for 190 SAs in inner core (IC), 168 SAs in outer core (OC) and 225 SAs in radial blanket (RB). The channel represents all axial segments of the 4300 mm height subassembly from the level of diagrid plate up to the outlet shielding sleeve:

- the inlet section (empty hexcan);
- pin bundle with associated heat structure;
- upper transition section (empty hexcan);
- outlet shielding section.

Pin parameters of fissile and fertile SAs and main thermal hydraulic parameters of the core at nominal operation are given in [14].

A simplified SA flow gagging scheme with three cooling groups is established which correspond to three core zones: IC, OC and RB. The cooling group mass flow rates were adjusted to achieve a similar average sodium heat-up of about 145°C in IC and OC at nominal operation conditions, while the sodium heat-up in RB subassemblies is set to somewhat lower value (up to 70°C in most powerful breeder SAs) [14].

The essential feature of the modelling in the current work is introduction of an additional number of heat structures and dedicated models in order to reproduce the reactivity effects related to thermal expansion of in-reactor structures. In addition to the heat structure of the control rod drive lines (CRDL), a diagrid and vessel structures are included in the model in order to account for the corresponding reactivity feedbacks. Dedicated models for strongback and fuel pellet stack expansion are also introduced. The feedbacks of vessel and strongback thermal expansion constitute a noticeable time delays, while neglecting of these effects may lead to inconsistent transient behaviour modelling.

### 3.3. Point kinetics neutronics model

A point kinetics (PK) model option in TRACE was used for calculation of the transient reactor power. The PK model considers approximation of the neutron flux by a product of fixed spatial shape function and time dependent multiplier, that allows to simplify neutron kinetics equations as following:

$$\frac{dn(t)}{dt} = \frac{\rho(t)-\beta_{eff}}{\Lambda} n(t) + \sum_k \lambda_k C_k(t), \quad (1)$$

$$\frac{dC_k(t)}{dt} = \frac{\beta_k}{\Lambda} n(t) - \lambda_k C_k(t), \quad (2)$$

where $n(t)$ – neutron density, 1/cm$^3$, proportional to reactor power; $\rho(t)$ – reactivity, unitless; $C_k(t)$ – delayed neutron precursor concentration in group *k*, 1/cm$^3$; $\beta_{eff}$ and $\beta_k$ – total and group effective delayed neutron fraction, unitless; $\lambda_k$ – decay constant for group *k*, 1/s; $\Lambda$ – neutron generation time, s.

The PK model is supplied with the power distribution, reactivity coefficients and kinetics parameters obtained from the static neutron physics simulation with the Serpent 2 Monte Carlo code [14,15]. The simulations employed the benchmark model, which includes detailed 3D description of the pin and subassembly geometry and composition [15]. The spatial power distribution is specified as average subassembly power for the three core zones and 16 axial nodes corresponding to the fuel height. For calculating the specific reactivity coefficients the core configuration at hot zero power (HZP) conditions (at 400°C) is taken as reference for branch calculations with perturbed core configurations. The reference configuration is characterized by control rods (CRs) inserted by about 40 cm.

The time-dependent transient reactivity $\rho$ is composed as following:

$$\rho = \rho_{Doppler} + \rho_{Sodium} + \rho_{Fuel} + \rho_{Clad} + \rho_{Diagrid} + \rho_{CRdiff}, \quad (3)$$

where the contributions are:

- $\rho_{Doppler}$ – fuel Doppler effect resulting from temperature broadening of the neutron cross section resonances and changes of the self-shielding effect for fuel isotopes;
- $\rho_{Sodium}$ – sodium density effect due to change of average sodium temperature in the core;

- $\rho_{Fuel}$ – fuel axial expansion effect, a reactivity feedback related to elongation or compaction of the fuel pellet stack height; the ”free” expansion of the fuel is considered, thus the effect is driven by average fuel temperature;
- $\rho_{Clad}$ – pin cladding material axial and radial expansion effect, driven by average cladding temperature;
- $\rho_{Diagrid}$ – diagrid plate radial expansion effect, due to change of subassembly pitch in the diagrid plate, which expands following core inlet temperature;
- $\rho_{CRdiff}$ - control rods differential position effect, defined from the following equation:

$$\rho_{CRdiff} = \delta_{CR} \cdot \left(\Delta H_{CRDL} + \Delta H_{Strongback} + \Delta H_{Vessel} + \Delta H_{Fuel}\right), \quad (4)$$

where $\delta_{CR}$ – control rods position reactivity worth, 1/mm; $\Delta H_{CRDL}$ – change of the CDRL length driven by average core outlet sodium temperature, mm; $\Delta H_{Strongback}$ – change of the core support structure (strongback) height driven by core inlet sodium temperature with a time delay, mm; $\Delta H_{Vessel}$ – change of the vessel height driven by core inlet sodium temperature with a time delay, mm; $\Delta H_{Fuel}$ – change of the fuel pellet stack height, mm, introducing a relative displacement of the fuel with respect to the control rods position.

Another specific effect, the subassembly pad effect [16], i.e. reactivity effect due to the thermal expansion of the pads between the hexcans leading to increase of the core radial dimension at the axial level of the pads (core flowering), was not considered due to high uncertainties of the modelling. This assumption should be reconsidered in future since the obtained difference between evaluated and experimental values of coefficient *g*, as was reported in [9], may be associated with this effect.

The set of coefficients used in [14] were revised and adopted for this study. The Doppler constant was derived considering the fuel isotopes temperature change from 600 K to 1500 K. Five individual contributions are derived for the fissile regions of IC and OC, lower and upper fertile blankets and RB. In addition, a ”cold” Doppler effect is taken into consideration in this study for the zero power conditions and core transition from 180°C to 400°C as described in [15]. Sodium density effect was modelled by variation of

sodium density within the hexcan at the fuel height. The fuel expansion is modelled assuming the fuel heat-up and corresponding “free” pellet stack elongation within the pin cladding (open gap regime as assumption for non-irradiated fuel). The fuel expansion coefficient was derived using the average fissile fuel temperature. The cladding expansion effect is evaluated on basis of the average cladding temperature assuming clad heat-up and its axial and radial thermal expansion. The control rods differential position reactivity worth $\delta_{CR}$ was derived on basis of the CRs worth curve and assumed CRs position in the core at given power conditions.

## 4. CORE REACTIVITY BALANCE AT DIFFERENT CONDITIONS

In the first part of the study the core reactivity change during its transition from 180°C to nominal power was evaluated. The experimental data are reported in [9]. The reactivity change is presented from the critical state at 180°C to the full power. The measured core reactivity value was deduced from the comparison of the control rod positions.

### 4.1. Assumptions for core transition from 180°C to nominal power

In spite of availability of general description of tests, the detailed parameters of the core during this transition are not available. Thus number of assumptions was considered in this study assuming also keeping a simplicity of the model. There is a number of uncertain parameters, which were evaluated and adopted for given core conditions, such as inlet sodium temperature and flow rate, fuel-clad gap conductance, CR curtains (a curtain is one ring of CSD rods) positions and corresponding cumulative reactivity worth at different thermal and power conditions. Moreover, the simplified model does not include the secondary and tertiary circuit, thus the account for the dynamic response of these systems is not possible and any perturbations are treated in a simplified manner by manipulating with primary mass flow and inlet temperature. Following assumptions were considered:

#### *4.1.1. Inlet sodium temperature at cold plenum and mass flow*

There is no data available on variation of the inlet temperature and mass flow during power raise. Thus the first approximation applied is that for all power levels the inlet sodium temperature is set to 400°C. The sodium mass flow is set to 18.4% of nominal value of 16400 kg/s for the heating up the core from 180°C to 400°C at nearly zero power. The mass flow rate was assumed 39.6% at 20% of nominal power and linearly increasing to 100% at nominal power. Such assumption on inlet parameters results in exclusion of the inlet temperature related feedbacks like diagrid, strongback and vessel expansion from the reactivity balance for the transition from zero to 100% nominal power. While they are not excluded in the evaluation of the core transition from initial criticality at 180°C to hot zero power conditions at 400°C.

***4.1.2. Fuel-clad gap conductance:***

The fuel-clad gap conductance is the most uncertain parameter in the fuel temperature evaluation. In [17] the fuel pin mechanics modelling is stated to be essentially important and neglecting of fuel pin mechanics dynamic response for some transient scenarios showed no satisfactory results. In [9] it is stated that for the powers range from 50% to 100% nominal during the first power raise the reactivity balance monitoring gave a value lower than the calculation. This difference could be attributed to an incorrect assessment of the heat conductance of the gap between the fuel and clad, which is the most uncertain parameter in the fuel temperature evaluation. Some other contributions to reactivity balance with lower dynamics were important for prediction of the core reactivity transition during operation above 50% nominal power.

In the current study a simplified approach was proposed with set of gap conductance values which depend on the power as shown in Figure 3. The whole range of powers has been split in four ranges each with the constant value of fuel-clad gap conductance. These values were selected based on simple estimates, engineering judgment and iterative optimization of the overall agreement of the predictions with the measured data.

***4.1.3. Control rods worth:***

The evolution of CRs positions (as well as mutual curtains positions) in the large SPX core reported in [8] is highly uncertain especially using a simplified model. The initial critical position was evaluated at the level of 40 cm simultaneous insertion for all CRs (CSD) [5], while there is no information available on mutual curtain positions and resulting cumulative CRs worth. Furthermore, for the power raise a withdrawal of CRs should be considered in order to make the core critical to compensate loss of reactivity (mainly due to two negative components: the fuel Doppler effect and the fuel axial expansion effect). Thus an assumption was taken on dependency of the CRs worth on core thermal state and power level. The CRs worth for different power conditions is shown in Figure 4. The stepwise dependence for the same four power regions as for the gap conductance case was derived in accord with the S-curve calculated by the Serpent 2 Monte Carlo code [15]. The evaluated CRs worth ranges from 12 to 7 pcm/mm approximately corresponding to the CRs insertion from ~40 to ~20 cm. The CRs worth decreases with power raise as the CRs are more withdrawn.

**4.2. Results of modelling of reactivity balance**

In Figure 5 the calculated reactivity balance is presented along with the data measured at Superphènix during the start-up tests and calculation results obtained with the COREA code [9]. The information on the curve covers two condition domains: first, the lower boundary of reactivity values demonstrates the reactivity change from zero power at 180°C to 20% nominal power; secondly, the dependency of the reactivity on power is provided for the levels from 20% to 100% nominal with 10%-step.

The simplified model allowed predicting the transition from 180°C to 20% nominal power in two phases. During the first phase, an isothermal heating up of the core at nearly zero power was modelled with increase of inlet temperature performed in few reactivity steps. This transition requires a withdrawal of the CRs and insertion of about +650 pcm. For this transition a “cold” Doppler constant of 1332 pcm was applied, as evaluated in [5] for the core configuration with CRs inserted by 40 cm. At the end of this phase, further heating up of the core due to power increase up to 20%nominal was considered resulting in a new steady state after step-wise insertion of +280 pcm. The

two phases reactivity change of 930 pcm reasonably fits with experimental measurement being about 50 pcm lower. The COREA code prediction of about 1000 pcm deviates from the experimental value by about 20 pcm.

Further reactivity transition was considered assuming the same initial reactivity point at 20% nominal power as for the experimental curve. Satisfactory agreement is obtained for the whole power range, while the reactivity "jumps" at 70, 80 and 100% nominal power were not reproduced since the modelling is simplified and considers the fuel-clad gap which was not changed within the given power range. Additionally, the potential contribution to the reactivity balance of mutual CR curtain positions change can not be evaluated. The curve obtained with one Doppler constant for the whole power range tends to deviate slightly for the powers above 60-70% nominal. Application of the Doppler constant value decreased by 10% (from 1115 to 1000 pcm) for this power range improves the agreement. Practically it constitutes a typical uncertainty level on this parameter within 10% as well as a deviation from the logarithmic law may be observed.

## 5. REACTIVITY COEFFICIENTS

### 5.1. Procedure for evaluation of reactivity coefficients

The procedure of evaluation of the reactivity coefficients *k*, *g*, *h* during the start-up tests in three steps is described in [9]. These three reactivity coefficients were evaluated in the current study:

- $k = \frac{\partial \rho}{\partial T_i}$ (pcm/°C) is the change of reactivity due to the 1°C-change of the sodium inlet temperature with the power and sodium heatup fixed;
- $g = \frac{\partial \rho}{\partial \Delta T}$ (pcm/°C) is the change of reactivity due to the 1°C-change of the sodium heatup with power and inlet temperature fixed;
- $h = \frac{\partial \rho}{\partial P}$ (pcm/% nominal power) is the change of reactivity due to the 1%-change of the reactor nominal power with the inlet temperature and heatup fixed.

Three perturbation types were considered in accord to [9]:

1. Reactivity insertion of -50 pcm.

2. Inlet temperature decrease by 10°C which models the response of the primary circuit to the increase of secondary sodium mass flow.
3. Decrease of the primary sodium mass flow by 10%.

After each step a new steady state was obtained. The reactivity change between two steady states is expressed at given power level, while these three perturbations allow to solve the system of equations with respect to the coefficients:

$$k \cdot dT_i + g \cdot d\Delta T + h \cdot dP = d\rho_{CR}, \quad (5)$$

where $dT_i$ is the inlet temperature change, $d\Delta T$ is the change of the sodium heatup in the core, $dP$ is the power change and $d\rho_{CR}$ is the change of the reactivity.

This experimental procedure was performed at different power levels. Thus a corresponding set of calculation experiments was proposed in this study in order to evaluate these coefficients for the simplified core model and compare to the experimental data. The key feature of this calculation experiments is use of the same model parameters as were used in evaluation of the reactivity balance, presented in previous section. The power levels and core initial conditions were chosen taking into account the reported transients in [9] and [10].

**5.2. Three-step calculation experiment overview**

The evolution of core parameters in the three-step calculation experiment is discussed hereafter for the initial core power of 692 MW (about 23% of nominal) as an example case. The selected results are presented in Figure 6.

As result of the first step with reactivity insertion of -50 pcm, the power decrease leads to a decrease of the sodium heatup and fuel temperature. The major reactivity contributions counterbalancing the inserted reactivity up to the newly established steady state (up to 4000 s) are the positive ones of the Doppler and fuel axial expansion reactivity effects as well as the CR differential position effect. The latter composed of four components (see Section 3.3) is mainly due to the corresponding contraction of CRDL due to its cooling down with the decrease of the core outlet temperature and an additional withdrawal of CRs due to the fuel height contraction. The resulting CRs withdrawal of about 1.2 mm provides a positive CR differential effect.

In the second step ended with a new steady state at nearly 8000 s the decrease of the core inlet temperature by 10°C causes noticeable thermal response of the vessel, strongback and diagrid plate, resulting in a strong reactivity effect due to the CRs withdrawal. In addition to the CRDL contribution, two other contributions of the CR differential position effects plotted in Figure 6 plays important role at this step: the positive strongback axial expansion contribution, which acts with characteristic delay of about 100 s and the negative vessel expansion contribution with delay of about 360 s. The diagrid radial expansion reactivity effect is also not negligible due to the radial compaction of the core. All the thermal effects result in an insertion of the CRs.

The third step with the decrease of the primary sodium mass flow by 10% is characterised by a slight heating up of the core resulted in a negative response of Doppler and fuel axial expansion reactivity effects along with a small decrease of the CRDL-related contribution. The CRs are slightly withdrawn at the end of this last step with respect to the initial position at the experiment start.

**5.3. Results on reactivity coefficients**

The reactivity coefficients shown in Figure 7 were evaluated at three power levels. The first calculation experiment was performed at the initial power level of 692 MW with the initial core conditions evaluated from the three step transient reported in [9]. The second power level and the core conditions point correspond to those at the reactivity insertion transient performed at 1540 MW in [10]. The latter point is chosen artificially with the core conditions corresponding to 80% nominal power defined as described in Section 4.1.

The experimentally measured data and calculation results reported in [9] are also shown in Figure 7. The *k* coefficient is reproduced reasonably well for all powers practically within the estimated from [9] uncertainty of experimental data. For the coefficient *g* calculation results show a similar trend as in the calculations also reported in [9]. It decreases with power while a slight increase was experimentally observed. Nevertheless for the powers below 50% the agreement is reasonable. The coefficient *h* is also reasonably reproduced up to the middle power, while the trend differs for higher

powers. Slight improvement on this coefficient may be achieved applying the Doppler constant value decreased by 10%, whereas other coefficients are less affected. This fits to the results obtained in the previous section. Additionally the influence of the differential CR position reactivity effect is demonstrated for all coefficients. It can be stated that neglecting of this effect does not allow to reproduce the experimental data reasonably with considered simplified model.

All coefficients exhibit decreasing trend with power, due to a strong fuel Doppler contribution, which decreases with nearly logarithmic law on fuel temperature and respectively on power level. For the coefficient *g*, the experimental values shows slight increase, in contrast to calculated ones. As reported in [9], this experimental behaviour may be attributed to pad effect (assumed to be zero in calculations) or to expansion in parts of the structures where temperature distribution has not been properly measured or calculated. The calculated value for the coefficient *h* is higher than the experimental one in high power range. This effect may result from overestimated Doppler constant. Reported in [9] Doppler constant value equals to 1086±20%, thus exhibits high uncertainty. Another potential contribution is the CR position uncertainty. The decrease of CR worth value will lead to decrease of the coefficient. Finally, as reported in [9], the fuel relocation may play not negligible role in evaluation of these coefficients. Reactivity balance monitoring after experiments revealed changes in fuel structure (geometry), i.e., a difference in fuel-clad gap conductance under irradiation. Fuel temperature is closely connected to this parameter, hence, the Doppler effect and consequently the power coefficient *h*. As reported in [9], further study is needed with fuel behaviour models to calculate the restructuring and swelling phenomena according to the reactor operation history because the rise to full power was a series of separate runs at intermediate powers marked by shutdowns, which speed up the fuel restructuring rate. Practically, for given power level of 80% nominal, the proposed fissile fuel gap conductance value of 8000 $W/m^2$ K may appear overestimated, resulting in lower fuel temperature at this power level and stronger Doppler effect contribution in the coefficient.

## 6. CONCLUSIONS AND OUTLOOK

The developed simplified neutronic/thermal-hydraulic core model of the SPX core was reported to be able to reproduce reasonably the experimentally measured reactivity characteristics of the core: reactivity balance and reactivity coefficients *k*, *g*, *h* at different power levels. In spite of a number of highly uncertain parameters in the model, the assumptions proposed provide a consistent look at the core behaviour for a wide range of thermal conditions: from the cold isothermal state at 180°C at zero power to nominal power conditions. Specifically, it has been demonstrated that reactivity effects related to thermal expansion of in-reactor structures naturally having high uncertainties and complicated phenomenology for modelling, may be appropriately described with use of the simplified models. Further improvements to reproduce the experimental data would require more precise look in the following directions. First, the dynamic modelling of the fuel pin behaviour could provide more accurate results in evaluation of fuel-clad gap conductance and potentially improve the results for evaluated reactivity coefficients *k*, *g*, *h*. A further sensitivity analysis may include variation of pre-calculated reactivity characteristics, such as Doppler constant and fuel expansion reactivity coefficient. The simplified assumptions on dependency of CR worth value on power level could be replaced by more sophisticated models, accounting a realistic position of different CR curtains (rings), if this information would be available. The same can be addressed to unknown parameter of core inlet temperature, which could vary for different power levels. The SPX core model developed will be used for further analysis of a number of transients in the core performed as start-up tests as proposed in the transient part of the SPX benchmark activities [5].

## REFERENCES

[1] “Generation IV International Forum Annual Report 2019”, accessed November 2020, https://www.gen-4.org/gif/jcms/c_119034/gif-2019-annual-report.

[2] IAEA-TECDOC-1691, 2012, “Status of Fast Reactor Research and Technology Development”, IAEA TECDOC Series, Vienna, Austria.

[3] Guidez, J., and Prêle, G., 2017, “Superphenix: Technical and Scientific Achievements, Atlantis Press and the author(s), ISBN 978-94-6239-246-5.

[4] Mikityuk, K., Girardi, E., Krepel, J., Bubelis, E., Fridman, E., Rineiski, A., and Girault, N., 2017. “ESFR-SMART: new Horizon-2020 project on SFR safety”, In Int. Conf. on Fast Reactors and Related Fuel Cycle: Next Generation Nuclear Systems for Sustainable Development (FR17).

[5] Ponomarev, A., Bednarova, A., and Mikityuk, K., 2018, “New sodium fast reactor neutronics benchmark”, Proc. of PHYSOR 2018, Cancun, Mexico, April 22-26, 2018.

[6] Gourdon, J., Mesnage, B., Voitellier, and J. L., Suescun, M., 1990, ”An Overview of Superphénix Commissioning Tests”, Nuclear Science and Engineering, Vol. 106, No. 1, pp. 1-10.

[7] Flamenbaum, G., de Wouters, R., Le Bourhis, A., Newton, T., and Vambenepe, G., 1990, “Superphénix Core-Loading Strategy Using the Checkerboard Pattern,” Nuclear Science and Engineering, Vol. 106, No. 1, pp. 11-17.

[8] Gauthier, J. C., Cabrillat, J. C., Palmiotti, G., Salvatores, M., Giese, M., Carta M., and West, J. P., 1990, “Measurement and Predictions of Control Rod Worth”, Nuclear Science and Engineering, Vol. 106, No. 1, pp. 18-29.

[9] Vanier, M., Bergeonneau, P., Gauthier, J. C., Jacob, M., de Antoni, J., Gesi, E., Peerani P., and Adam, J. P., 1990, “Superphénix Reactivity Feedback and Coefficients”, Nuclear Science and Engineering, Vol. 106, No. 1, pp. 30-36.

[10] Bergeonneau, Ph., Vanier, M., Favet, M., De Antoni, J., Essig, K., and Adam, J. P., 1990, ”An Analysis of the Dynamic Behavior of the Core”, Nuclear Science and Engineering, Vol. 106, No. 1, pp. 69-74.

[11] Mikityuk, K. Pelloni, S., Coddington, P., Bubelis, E., and Chawla., R., 2005, "FAST: An Advanced Code System for FAST Reactor Transient Analysis," Annals of Nuclear Energy, Vol. 32, pp. 1613-1631.

[12] Mikityuk, K., Krepel, J., Pelloni, S., Girardin, G., Chenu, A., Sun, K., Alonso, M., Marinoni, A., Adams, R., Reiterer, F., and Monti, S. (Ed.), 2015, “Fast Code System: Review of Recent Applications,” International Atomic Energy Agency (IAEA).

[13] Leppanen, J., Pusa, M., Viitanen, T., Valtavirta, V., and Kaltiaisenaho, T., 2015, “The Serpent Monte Carlo code: Status, development and applications in 2013”, Annals of Nuclear Energy, Vol. 82, pp. 142-150.

[14] Ponomarev, A., and Mikityuk, K., 2019, ”Analysis of hypothetical Unprotected Loss Of Flow in Superphénix start-up core: sensitivity to modeling details”, Proc. of the 27th International Conference on Nuclear Engineering (ICONE-27), The Japan Society of Mechanical Engineers.

[15] Ponomarev, A., Mikityuk, K., Zhang, L., Nikitin, E., Fridman, E., Álvarez-Velarde, F., Romojaro Otero, P., Jiménez-Carrascosa, A., García-Herranz, N., Lindley, B., Davies, U., Seubert, A., and Henry, R., 2021, “SPX Benchmark Part I: Results of Static Neutronics,” Journal of Nuclear Engineering and Radiation Science, Vol. Accepted.

[16] Bernard, A., Masoni, P., Van Dorsselaere, J.P., 1983, ”Mechanical Behavior of a Fast Reactor Core. Application of the 3D Codes to SUPERPHENIX 1”, IASMiRT Report, Chicago, USA, August 22-26, 1983, http://www.lib.ncsu.edu/resolver/1840.20/25859.

[17] Mikityuk, K., and Schikorr, M., 2013, “New Transient Analysis of the Superphénix start-up Tests”, Proceedings of International Conference on Fast Reactors and Related Fuel Cycles: Safe Technologies and Sustainable Scenarios (FR’13), Paris, France, March 4-7, 2013.

## FUNDING

The work has been supported within EU Project ESFR-SMART which has received funding from the EURATOM Research and Training Programme 2014-2018 under the Grant Agreement No. 754501.

**NOMENCLATURE**

| | |
|---|---|
| $C_k$ | delayed neutron precursor concentration in group *k*, 1/cm$^3$ |
| *g* | reactivity coefficient related to change of the sodium heat-up, pcm/°C |
| *h* | reactivity coefficient related to change of the core power, pcm/% nominal power |
| $\Delta H_{Fuel}$ | change of the fuel pellet stack height, mm |
| $\Delta H_{CRDL}$ | change of the CDRL length, mm |
| $\Delta H_{Strongback}$ | change of the strongback height, mm |
| $\Delta H_{Vessel}$ | change of the vessel height, mm |
| *k* | reactivity coefficient related to change of the sodium inlet temperature, pcm/°C |
| *n* | neutron density, 1/cm$^3$ |
| $P$ | core power, W or % nominal power |
| *t* | time, s |
| $\Delta T$ | sodium heat-up in the core, °C |
| $T_i$ | sodium inlet temperature, °C |

**Greek letters**

| | |
|---|---|
| $\beta_{eff}$ | total effective delayed neutron fraction, unitless or pcm |
| $\beta_k$ | group *k* effective delayed neutron fraction, unitless or pcm |
| $\delta_{CR}$ | control rods position reactivity worth, 1/mm or pcm/mm |

| | |
|---|---|
| $\lambda_k$ | decay constant for group *k*, 1/s |
| $\Lambda$ | neutron generation time, s |
| $\rho$ | reactivity, unitless or pcmType equation here. |
| $\rho_{Clad}$ | cladding expansion reactivity, unitless or pcm |
| $\rho_{CR}$ | reactivity change due to moving the control rods, unitless or pcm |
| $\rho_{CRdiff}$ | differential control rod position reactivity, unitless or pcm |
| $\rho_{Diagrid}$ | diagrid plate radial expansion reactivity, unitless or pcm |
| $\rho_{Doppler}$ | fuel Doppler reactivity, unitless or pcm |
| $\rho_{Fuel}$ | fuel axial expansion reactivity, unitless or pcm |
| $\rho_{Sodium}$ | sodium density reactivity, unitless or pcm |

Type equation here.

**Acronyms and abbreviations**

| | |
|---|---|
| 3D | Three Dimensional |
| CR | Control Rod |
| CRDL | Control Rod Drive Line |
| CSD | Control and Shutdown Device |
| DSD | Diverse Shutdown Device |
| GFR | Gas cooled Fast Reactor |
| HZP | Hot Zero Power |

| | |
|---|---|
| IC | Inner Core |
| MOX | Mixed Oxide (nuclear fuel) |
| MSR | Molten Salt cooled Reactor |
| OC | Outer Core |
| pcm | per cent mille or $10^{-5}$ (is equal to one-thousandth of a percent of the reactivity) |
| PK | Point Kinetics |
| RB | Radial Blanket |
| SA | SubAssembly |
| SFR | Sodium cooled Fast Reactor |
| SPX | French sodium cooled fast reactor Superphénix |
| US NRC | United States Nuclear Regulatory Commission |

## Figure Captions List

## Table Caption List

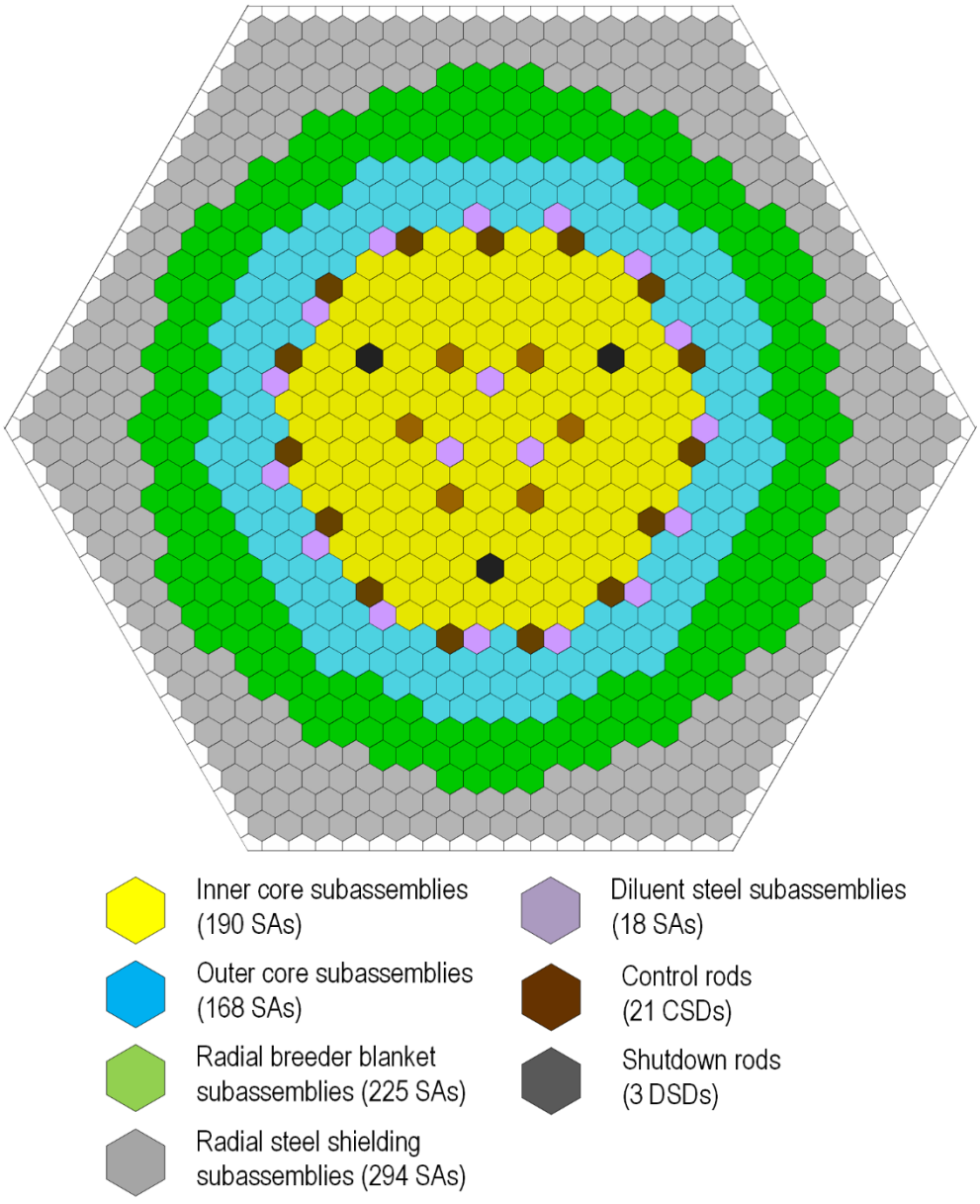


Figure 1. Subassembly arrangement of start-up SPX core configuration

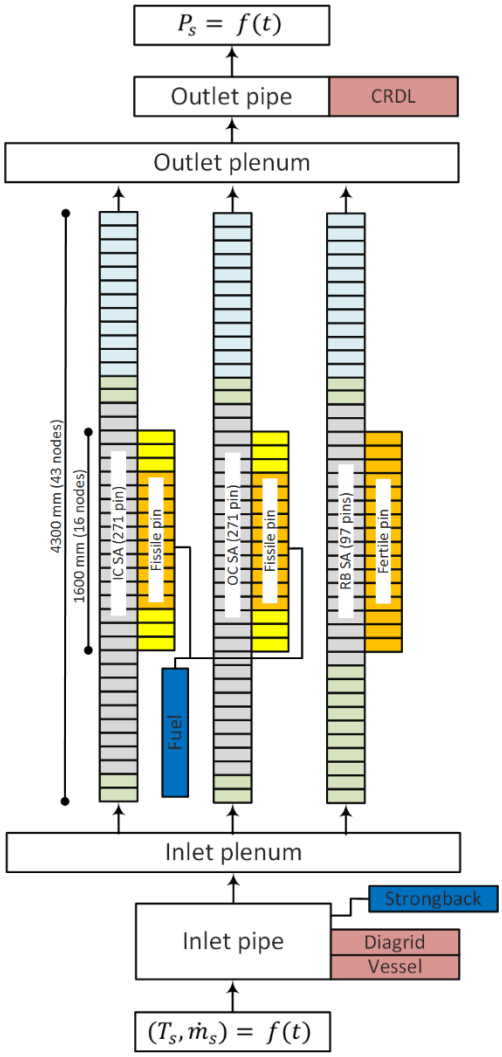


Figure 2. TRACE model of SPX core

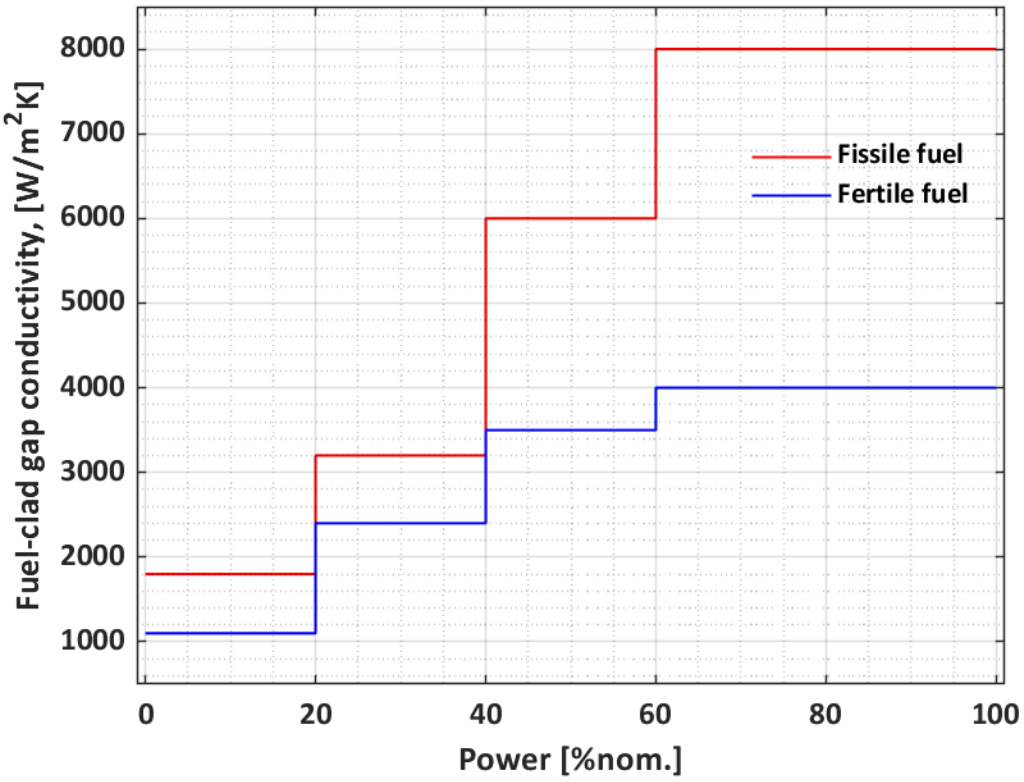


Figure 3. Fuel-clad gap conductance at different power levels

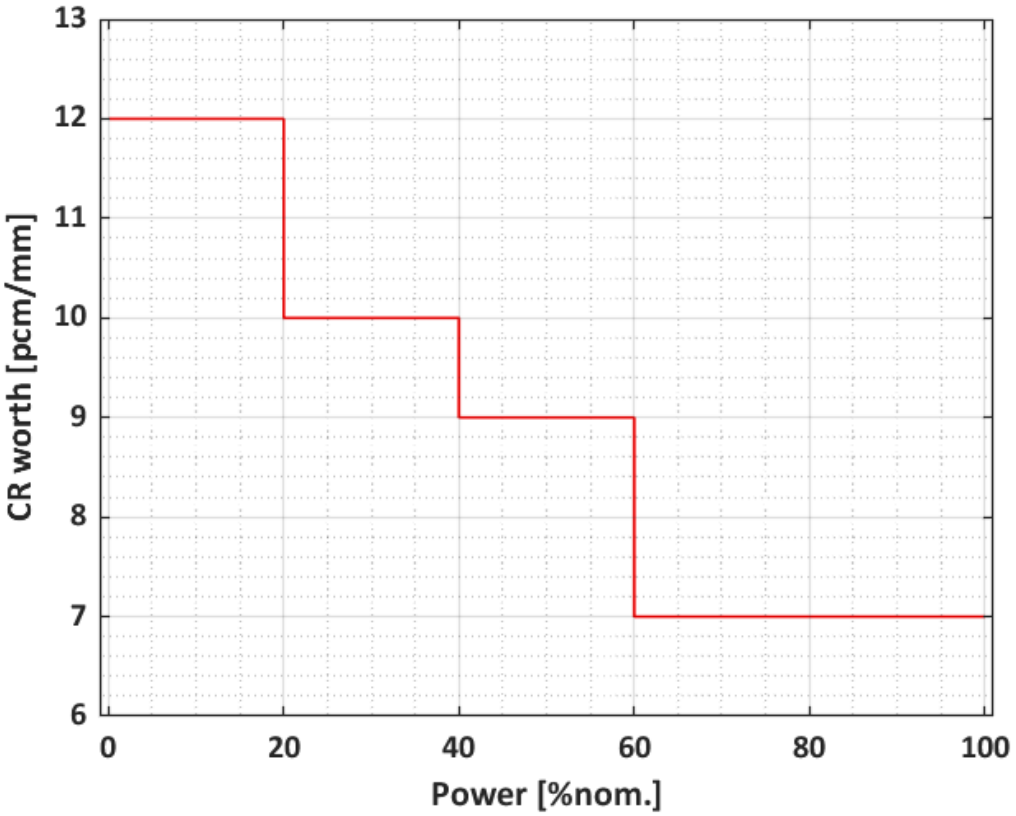


Figure 4. CRs worth at different power levels

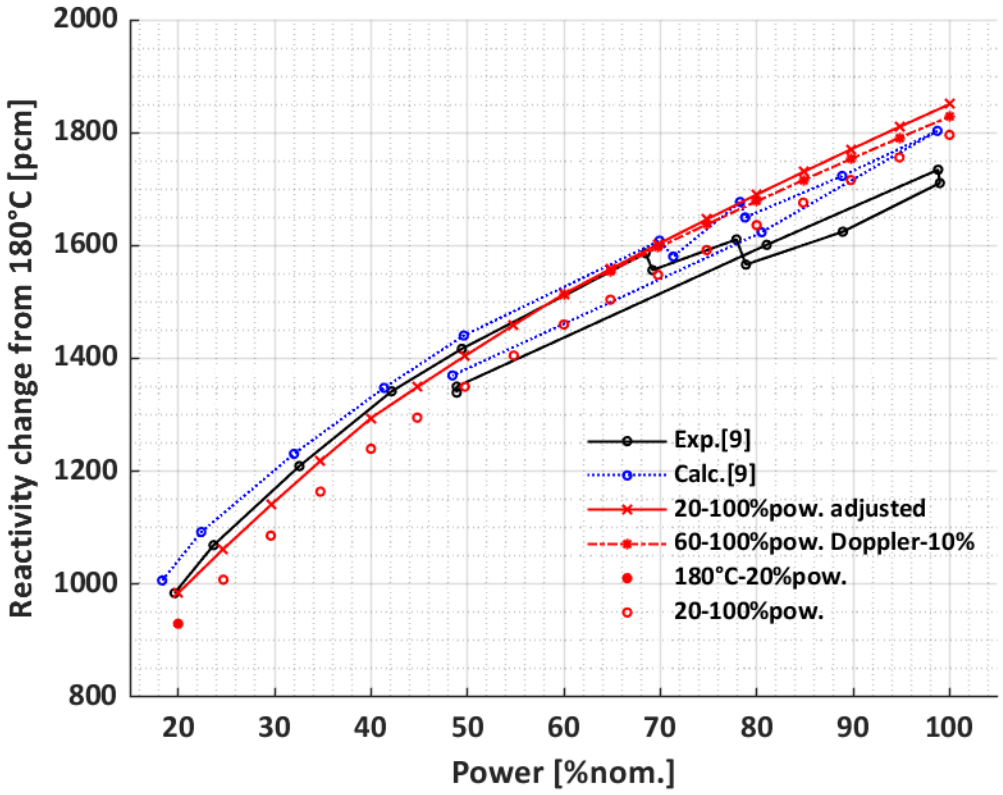


Figure 5. Reactivity balance at different power levels

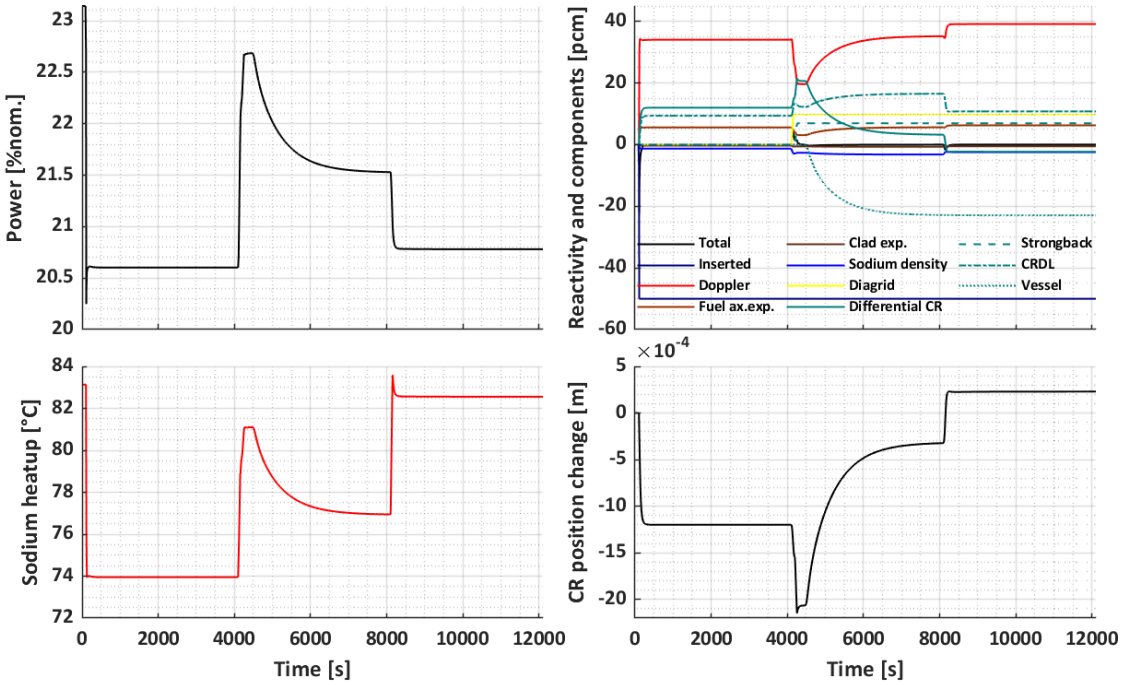


Figure 6. Evolution of selected parameters in three-step calculation experiment at 692 MW

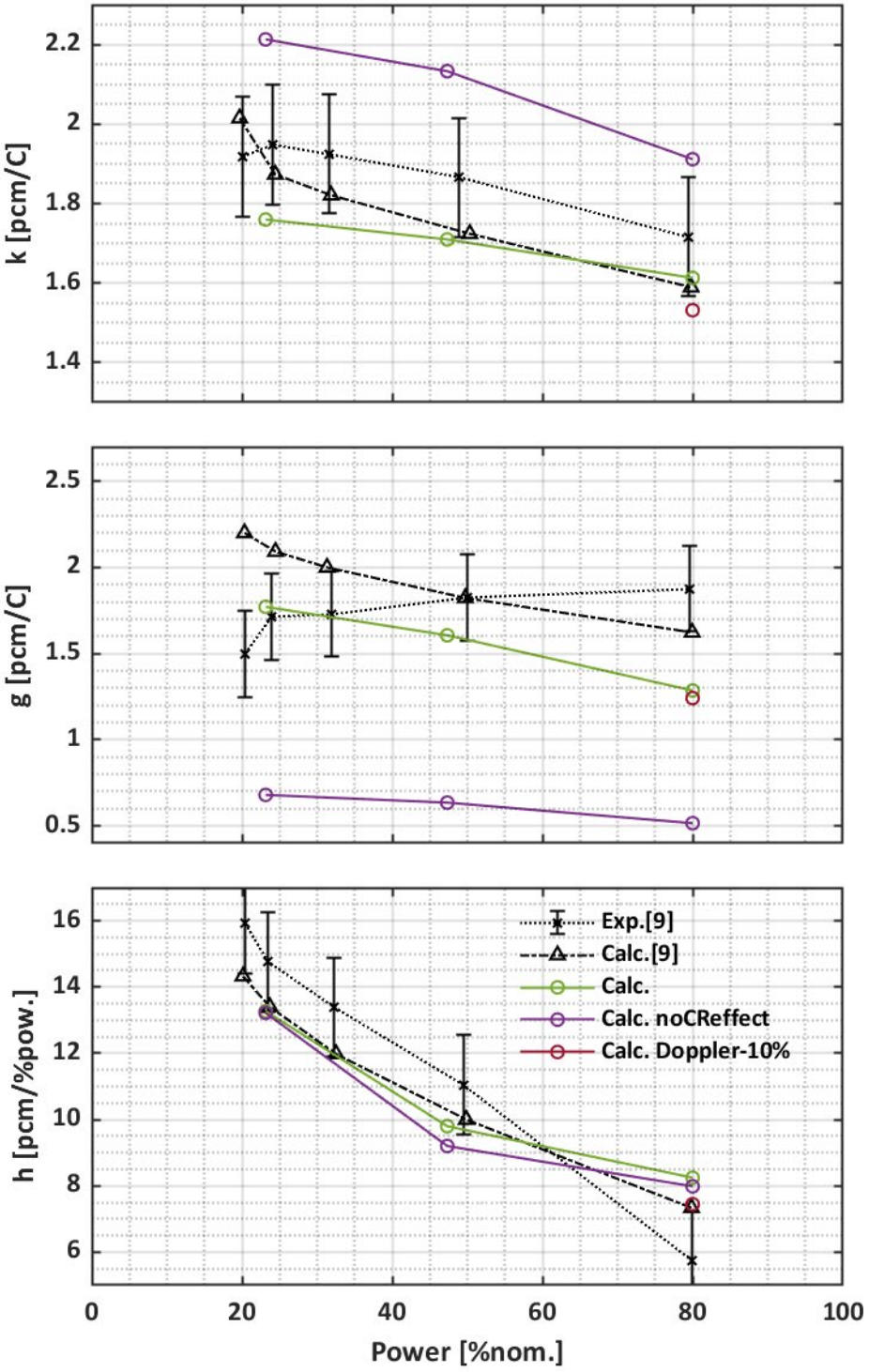


Figure 7. Reactivity coefficients *k*, *g* and *h* at different power levels

Table 1. Selected parameters of SPX reactor [2,6]

| Parameter | Value |
|---|---|
| Thermal/electric power | 3000 / 1240 MW |
| Average fissile/fertile fuel temperature | 1227/627°C |
| Primary sodium inlet/outlet temperature | 395/545°C |
| Primary sodium mass flow | 16400 kg/s |
| Fissile/fertile fuel | $(U,Pu)O_2/UO_2$ |
| Plutonium content in inner/outer core zones | 16.0/19.7% |
| Total mass of plutonium in the fissile core | 5780 kg |
| Volume of the fissile core | 10.8 $m^3$ |
| Equivalent diameter of the fissile core | 3.70 m |
| Height of the fissile pellet stack | 1.00 m |
| Height of the lower/upper breeder blankets | 0.30/0.30 m |
| Height of the radial blanket fertile pellet stack | 1.60 m |
| Subassembly pitch | 179.0 mm |
| Number of SAs in inner core/outer core/radial blanket | 190/168/225 |
| Number of control rods (CSD/DSD) | 21/3 |